

Depth-selective measurements of induced magnetic polarization in Cu layers of Gd/Cu multilayers by ^{119}Sn Mössbauer spectroscopy

This article has been downloaded from IOPscience. Please scroll down to see the full text article.

2005 J. Phys.: Condens. Matter 17 4023

(<http://iopscience.iop.org/0953-8984/17/26/003>)

View [the table of contents for this issue](#), or go to the [journal homepage](#) for more

Download details:

IP Address: 129.252.86.83

The article was downloaded on 28/05/2010 at 05:12

Please note that [terms and conditions apply](#).

Depth-selective measurements of induced magnetic polarization in Cu layers of Gd/Cu multilayers by ^{119}Sn Mössbauer spectroscopy

T Ohkochi¹, N Hosoi² and K Mibu³

¹ Institute for Chemical Research, Kyoto University, Uji, Kyoto, 611-0011, Japan

² Research and Education Center for Materials Science, Nara Institute of Science and Technology, Ikoma, Nara, 630-0192, Japan

³ Research Center for Low Temperature and Materials Sciences, Kyoto University, Uji, Kyoto, 611-0011, Japan

E-mail: takuo@ssc1.kuicr.kyoto-u.ac.jp

Received 13 October 2004, in final form 10 May 2005

Published 17 June 2005

Online at stacks.iop.org/JPhysCM/17/4023

Abstract

We performed ^{119}Sn Mössbauer spectroscopic measurements on Gd/Cu multilayers with ^{119}Sn probing atoms. The Cu layers are delta-doped with Sn probes at a certain depth. Hyperfine fields are observed in the Mössbauer spectra at low temperatures below the Curie temperature of the Gd layers. From the temperature-dependent measurements, the hyperfine field is found to be proportional to the spontaneous magnetization of the Gd layer. The result indicates that the Gd magnetization induces magnetic polarization in the Cu layers. The hyperfine field per Gd magnetization is found to be $\sim 40 \text{ kOe}/\mu_{\text{B(Gd)}}$, regardless of the position of the ^{119}Sn atoms and the Cu thickness (20–40 Å), suggesting that the magnetic polarization in the Cu layer is uniform at any depth from the Gd/Cu interface.

1. Introduction

One of the most fascinating properties of ferromagnetic/nonmagnetic metallic layered systems is oscillatory exchange coupling between adjacent magnetic layers [1–4]. The strength and oscillation period of the interlayer exchange coupling for various systems have been revealed by probing macroscopic magnetization of the ferromagnetic layers. These experimental results are supported by theoretical studies [5, 6]. Since the interlayer exchange coupling is mediated by small magnetic polarization (spin polarization) induced in the nonmagnetic spacer layers, investigation on the magnetism of the nonmagnetic layers is a subject of great importance for the elucidation of interlayer magnetic coupling.

Recently, various methods have been used to probe small magnetic polarization induced in nonmagnetic spacers [7–16]. However, no general consensus has been obtained on the ‘size’

and ‘profile (depth distribution)’ of the induced magnetic polarization in the nonmagnetic layers. Even the penetration depth of the induced spin polarization in nonmagnetic layers has not been shown clearly. In fact, experimental methods to obtain depth-resolved magnetic polarization in nonmagnetic spacers are limited. Earlier works using NMR spectroscopy [11], the muon spin rotation (μ SR) technique [12], and so on, found oscillatory magnetic polarization in the nonmagnetic layers. Nevertheless, these methods simply infer the distribution from the integrated magnetic signal of the whole nonmagnetic layer. Low-angle x-ray diffraction measurement using the resonant magnetic scattering effect [13, 14] can estimate the profile of magnetization distribution of specific elements by observing the Fourier components of magnetic modulation and is a promising method to obtain the depth profile of magnetic polarization. ^{119}Sn Mössbauer spectroscopy can observe the induced magnetic polarization of the nonmagnetic layers depth-selectively as a hyperfine field of the Sn probing atoms when the nonmagnetic layers are delta-doped with nonmagnetic ^{119}Sn atoms in an appropriate position [15, 16].

We have been studying Gd/Cu systems to investigate the relationship between the magnetic polarization of the Cu layers and the size of the magnetization of the Gd layers. The use of Gd instead of 3d magnetic metals makes it possible to change the size of the magnetization by simply cooling the sample, because Gd has a Curie temperature of ~ 293 K in the bulk. Our previous work on Gd/Cu multilayers using hard x-ray magnetic circular dichroism (XMCD) measurements [17] at various temperatures revealed that the induced magnetic polarization in the 4p level of the Cu layers is proportional to the Gd magnetization. The result also suggested that the depth profile of the induced magnetic polarization scaled to the Gd magnetization is unchanged when the Gd magnetization varies in size.

In this paper, we present the results of Mössbauer measurements on Gd/Cu multilayers with ^{119}Sn probing atoms in Cu layers to estimate the attenuation of the Cu polarization as a function of the distance from the Gd/Cu interface and temperature. The magnetic polarization of the Cu layers is investigated via a hyperfine field of Sn probes, which is proportional to the s-electron polarization at the Sn nucleus position. We found that the scaled hyperfine field per Gd magnetization was constant, independent of the Cu thickness (20–40 Å) and the depth of the ^{119}Sn probes.

2. Experimental details

The samples were prepared by electron beam deposition in an ultrahigh-vacuum chamber. Multilayers were grown on polyimide substrates at room temperature. The basic layer structure is substrate/[Gd(t_{Gd})/Cu(t_{Cu})]₃₀/Gd(t_{Gd})/Si(50 Å)($t_{\text{Gd}} = 60, 100$ Å, $t_{\text{Cu}} = 20\text{--}40$ Å). Nominally half a monolayer (ML) of ^{119}Sn probes (1 Å) are embedded at a certain depth in the Cu layers. The Si layer on the top of the film is to protect Gd against oxidation. Macroscopic magnetizations were measured by a SQUID magnetometer. The interfacial and crystalline structures of the samples were characterized by x-ray diffraction and extended x-ray absorption fine structure (EXAFS) measurements. The EXAFS spectrum of the Gd/Cu sample grown on polyimide film was collected on the 4ID-D beamline at Advanced Photon Source, Argonne National Laboratory. Measurements were carried out in a transmission geometry.

We applied XMCD spectroscopy near the Cu K-edge to Gd/Cu multilayers with and without ^{119}Sn probes to examine the influence of embedded ^{119}Sn atoms on the magnetic polarization of Cu atoms. Measurements were performed at the BL39XU beamline in SPring-8 (Japan Synchrotron Radiation Research Institute). The detailed experimental procedure and the features of Cu-K XMCD spectra of the Gd/Cu systems without Sn are described elsewhere [17].

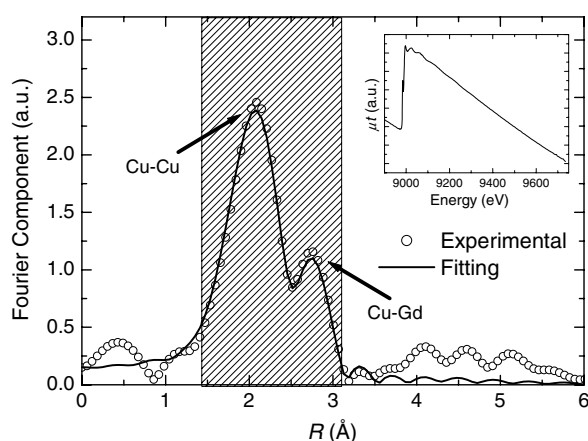


Figure 1. Magnitude of the Fourier transform of the EXAFS spectrum above the Cu K-edge on the $[\text{Gd}(60 \text{ \AA})/\text{Cu}(20 \text{ \AA})]_{15}$ multilayer. The inset shows the raw EXAFS spectrum.

Transmission ^{119}Sn Mössbauer measurements were carried out with a $^{119\text{m}}\text{Sn}$ γ -ray source in a CaSnO_3 matrix. A velocity transducer was operated in a constant acceleration mode. Samples grown on polyimide films were folded into a $15 \times 15 \text{ mm}^2$ square and mounted in a cryostat with which we can control the sample temperatures between 17 and 295 K. Transmitted γ -rays were detected by a proportional counter and recorded by a multichannel analyser. The channel number was converted to Doppler velocity by referring to the ^{57}Fe Mössbauer spectrum of standard α -Fe. The isomer shift of the Sn spectrum is shown relative to that of CaSnO_3 at room temperature. Magnetic splittings of the ^{119}Sn Mössbauer spectrum prove the existence of magnetic polarization at the atoms surrounding the Sn probing atom. We estimated the relative size of the magnetic polarization on Cu atoms depth-selectively by inserting ^{119}Sn probes at a known depth in the Cu layers of Gd/Cu multilayers and observing the hyperfine field at the Sn sites.

3. Sample characterization

The low-angle x-ray reflectivity profiles on our samples, which were grown on the substrates at room temperature, showed superlattice Bragg peaks up to the 3–4th order, indicating that the layered structure is formed well and that the intermixing is limited to the interface. The reflectivity profiles are similar to that collected on a polycrystalline Fe/Gd multilayer [13]. The interface structures seem to become slightly rougher by inserting ^{119}Sn probes. The Bragg peaks have completely vanished in the case of Gd/Cu samples grown on 200°C , due to alloying.

Figure 1 shows the magnitude of the Fourier transform of the EXAFS spectrum above the Cu K-edge collected on the polyimide/ $[\text{Gd}(60 \text{ \AA})/\text{Cu}(20 \text{ \AA})]_{15}$ multilayer, together with the raw absorption spectrum in the inset. In the figure, two peaks indicative of Cu–Cu bonding ($R = 2.46 \text{ \AA}$) and Cu–Gd bonding ($R = 2.88 \text{ \AA}$) are observed (see table 1). We estimated the coordination numbers of Cu and Gd atoms around the Cu atom by fitting, assuming that the total coordination number is nearly 12, as expected for an fcc or hcp crystal. The ratio of the coordination numbers $N_{\text{Cu–Cu}}:N_{\text{Cu–Gd}}$ is roughly 4:1, as seen in table 1. Assuming that the sample consists of ideally flat $[\text{Gd}/\text{Gd}_{50}\text{Cu}_{50}/\text{Cu}/\text{Gd}_{50}\text{Cu}_{50}]$ layers with $N_{\text{Cu–Cu}} \sim 6$ and $N_{\text{Cu–Gd}} \sim 6$ for the $\text{Cu}_{50}\text{Gd}_{50}$ alloy layer and $N_{\text{Cu–Cu}} \sim 12$ for the pure Cu layer, the thicknesses estimated from the ratio of the coordination numbers

Table 1. Fitting parameters (coordination numbers and distances) of the radial distribution function of the EXAFS spectrum shown in figure 1.

	Cu–Cu	Cu–Gd
Coordination number	8.74 ± 0.82	2.20 ± 0.46
Distance (Å)	2.46 ± 0.02	2.88 ± 0.03

are [Gd(52 Å)/Cu₅₀Gd₅₀(8 Å)/Cu(12 Å)/Cu₅₀Gd₅₀(8 Å)]. In this model, roughly 4 Å (2 monolayers) of interface Cu participate in alloying. Since the uneven interface also increases the amount of Cu–Gd bonding, the thickness of the Gd–Cu alloy layer may be thinner in the actual sample.

The high-angle x-ray diffraction patterns suggest that the Gd and Cu layers have microcrystalline or mostly amorphous structures. The intensity of the diffraction peaks indicative of Gd hcp structure gets weaker with increasing Cu thickness.

Magnetization measurements indicated that the amorphous-like Gd layers have significantly lower Curie temperatures in comparison with bulk Gd (293 K) [17]. (The temperature dependence of spontaneous magnetization is shown later in figures 4–6, together with that of the hyperfine field.) The [Gd(60 Å)/Cu(20 Å)]₃₀ multilayer shows a Curie temperature of ~120 K. The Curie temperature and saturation magnetization of the Gd/Cu multilayers reduce systematically when the Cu spacer becomes thicker, even if the Gd thickness is fixed. The reason for these systematic tendencies is thought to be a change in crystallinity of the Gd layers, not a formation of Gd–Cu alloy. The relationship between Curie temperature and crystalline structure of thin Gd layers is also discussed by Vas'kovskiy *et al* [18]; in the [Gd(150 Å)/Cu(20 Å)] and [Gd(150 Å)/Si(20 Å)] multilayers, the T_C values of the amorphous and crystalline phases of Gd are ~130 and ~290 K, respectively. The ratio of higher T_C phase of Gd/Si increases by annealing due to the improvement of crystallinity, whereas the T_C of Gd/Cu decreases due to the formation of Gd–Cu alloy. The Gd/Cu systems did not show oscillatory magnetic coupling or giant magnetoresistance effect.

4. Results and discussion

Figure 2 shows the x-ray absorption spectra (XAS) and the XMCD spectra at 20 K on four samples whose structures are [Gd(60 Å)/Cu(20 Å)]₃₀ and [Gd(60 Å)/Cu(z)/Sn(1 Å)/Cu(20 Å – z)]₃₀ ($z = 0, 5, \text{ and } 10 \text{ Å}$). The intensities of the XMCD signals are shown relative to the absorption step height of XAS signals (μt_{jump} in the figure) and are normalized to the Gd magnetization ($\mu_{B(\text{Gd})}$) measured by a SQUID magnetometer. The signal intensity and the shape of the XMCD spectrum for the sample without Sn probes are almost the same as those of the samples with Sn probes at different depths. The existence of Sn atoms does not seem to change the magnetism of the Cu layers significantly. From these facts, we safely regard the ¹¹⁹Sn Mössbauer nuclei as good probes to study the magnetic polarization of the Cu layers in Gd/Cu multilayers.

Figure 3 shows (a) the ¹¹⁹Sn Mössbauer spectra at several temperatures on three samples with $t_{\text{Cu}} = 20 \text{ Å}$ whose structures are [Gd(60 Å)/Cu(z)/Sn(1 Å)/Cu(20 Å – z)] ($z = 0, 5, \text{ and } 10 \text{ Å}$), together with the results of least-squares-fitting and (b) the distribution of hyperfine fields. In figure 4, the average hyperfine fields of Sn at several temperatures estimated from the distribution of hyperfine fields are plotted. Since the Mössbauer spectra were measured in zero field, the temperature dependence is compared with the spontaneous magnetizations (M_{sp}) of the Gd layers, which were estimated from the Arrot plot of the magnetization curves.

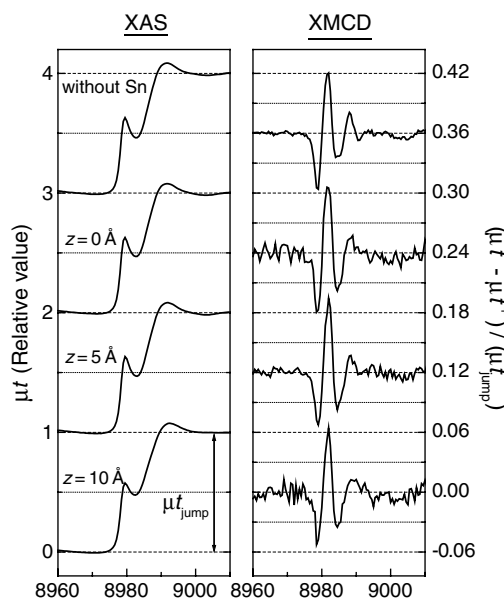


Figure 2. XAS and XMCD spectra on [Gd(60 Å)/Cu(20 Å)] and [Gd(60 Å)/Cu(z)/Sn(1 Å)/Cu(20 Å - z)] ($z = 0, 5, \text{ and } 10 \text{ \AA}$) samples. The size of the XMCD difference signals is expressed relative to the absorption step height (μt_{jump}) and is normalized to the Gd magnetization (μ_{Gd}).

The spontaneous magnetization versus temperature curves for these samples are shown so as to fit the average hyperfine fields.

At 20 K, each sample exhibits a very large average hyperfine field of ~ 250 kOe. The Mössbauer spectra for three samples have similar shape and similar hyperfine field distribution, although the ^{119}Sn atoms in these samples are embedded at different depths in the Cu layers. Each spectrum has a narrow distribution of the hyperfine field, and we can distinguish six peaks in the spectrum. For each sample, the average hyperfine field reduces as the temperature is raised, and it has good proportionality with the values of spontaneous magnetization of the Gd layer, as seen in figure 4. The proportional constants (average hyperfine field)/(Gd magnetization) estimated by least-squares fitting are shown in the figure. The values of hyperfine field per Gd magnetization are 42.2, 42.7, 39.5 kOe/ $\mu_{\text{B(Gd)}}$ for the samples with $z = 0, 5, 10 \text{ \AA}$, respectively. The slight difference of ~ 3 kOe/ $\mu_{\text{B(Gd)}}$ is within the evaluation error of each sample. At intermediate temperatures, the average hyperfine field is slightly larger for the sample with ^{119}Sn probes in the middle of the Cu layer ($z = 10 \text{ \AA}$). This tendency becomes apparent near the Curie temperature, i.e., at 90 K. The magnetization measurements show that these samples have slightly different Curie temperatures and saturation magnetizations. The ^{119}Sn probes seem to reduce the macroscopic magnetization of Gd when they are embedded near the interfaces. Nevertheless, the proportionality between the average hyperfine field and the Gd magnetization holds true at any temperature for all samples. No salient features are found from the isomer shift; the value is practically the same, $\sim 1.9 \text{ mm s}^{-1}$, for all samples, and only changes slightly by changing temperature due to the second-order Doppler shift.

Figures 5(a) and 6(a) show the ^{119}Sn Mössbauer spectra and hyperfine field distribution on three samples with thicker Cu layers ($t_{\text{Cu}} = 30, 40 \text{ \AA}$), i.e., [Gd(60 Å)/Cu(15 Å)/Sn(1 Å)/Cu(15 Å)]₃₀ and [Gd(100 Å)/Cu(z)/Sn(1 Å)/Cu(40 Å - z)]₃₀ ($z = 10$ and

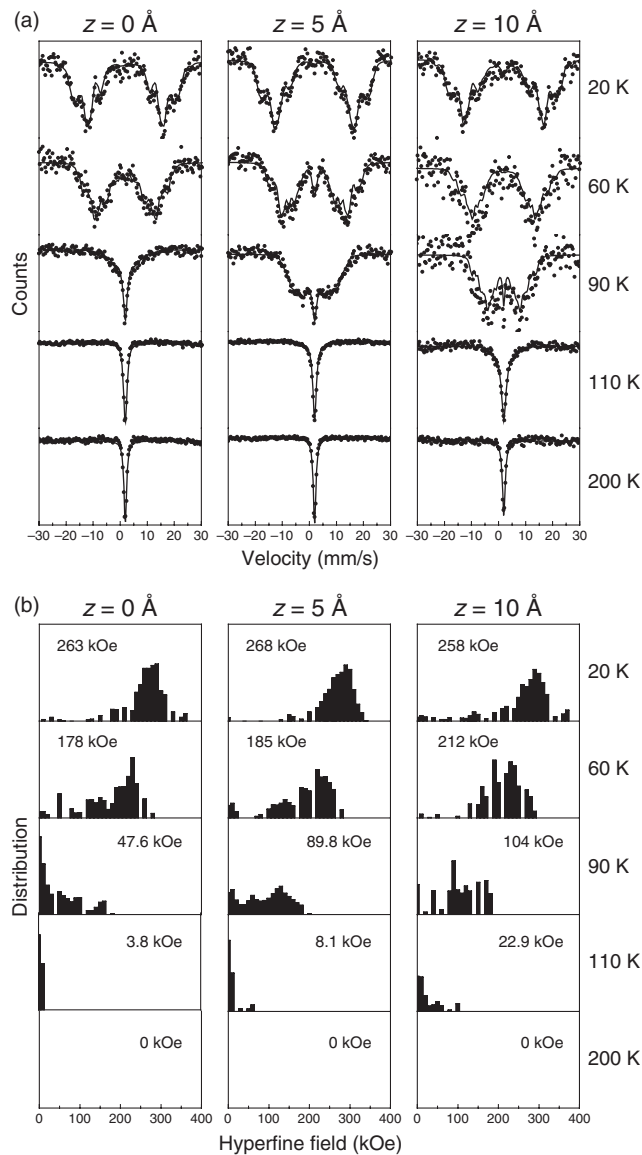


Figure 3. (a) ^{119}Sn Mössbauer spectra on $[\text{Gd}(60 \text{ \AA})/\text{Cu}(z)/\text{Sn}(1 \text{ \AA})/\text{Cu}(20 \text{ \AA} - z)]$ ($z = 0, 5, \text{ and } 10 \text{ \AA}$) samples (circular dots) and the fitting curves (solid lines) at several temperatures. (b) Distribution of hyperfine field corresponding to the fitting curves of (a). The values of the average hyperfine field are also shown.

20 Å). As mentioned in section 3, the Curie temperature and saturation magnetization reduce systematically when the Cu thickness increases even when the Gd thickness is fixed. When the Cu thickness becomes larger, and reaches $\sim 40 \text{ \AA}$, a Gd thickness of $\sim 100 \text{ \AA}$ is required to obtain a saturation magnetization and a Curie temperature comparable to those of the $[\text{Gd}(60 \text{ \AA})/\text{Cu}(20 \text{ \AA})]$ sample. In $[\text{Gd}(60 \text{ \AA})/\text{Cu}(15 \text{ \AA})/\text{Sn}(1 \text{ \AA})/\text{Cu}(15 \text{ \AA})]_{30}$, the average hyperfine fields are smaller at any temperature than those of the sample with $t_{\text{Cu}} = 20 \text{ \AA}$ because the Gd magnetization is smaller. Other features, such as the spectral shapes, the

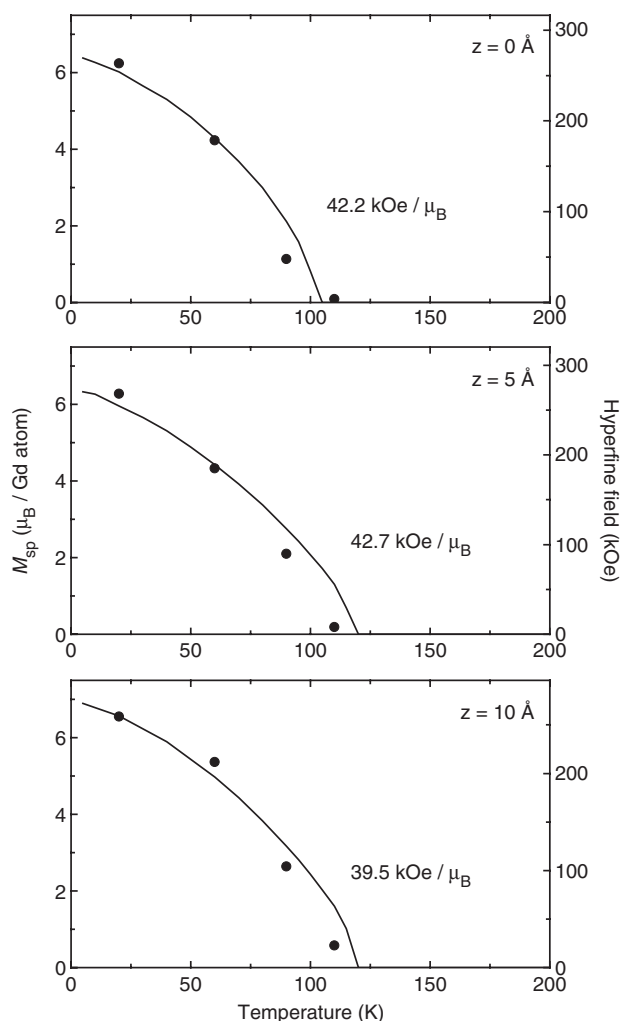


Figure 4. Temperature dependence of the average hyperfine field (circular dots) and spontaneous magnetization (M_{sp}) versus temperature curves (solid lines) for $[\text{Gd}(60 \text{ \AA})/\text{Cu}(z)/\text{Sn}(1 \text{ \AA})/\text{Cu}(20 \text{ \AA} - z)]$ ($z = 0, 5, 10 \text{ \AA}$) samples. The values of the hyperfine field per Gd magnetization are also shown.

distribution of hyperfine field at each temperature, and the isomer shifts, are also similar to those of the samples with $t_{\text{Cu}} = 20 \text{ \AA}$. The plots of average hyperfine field versus temperature and spontaneous magnetization versus temperature curves are shown in figures 5(b) and 6(b). For all samples, the average hyperfine fields are proportional to the Gd magnetization at any temperature. The average hyperfine fields per $1 \mu_{\text{B}}$ of Gd are 38.0, 39.0 and 39.9 $\text{kOe}/\mu_{\text{B}(\text{Gd})}$ for $[\text{Gd}(60 \text{ \AA})/\text{Cu}(15 \text{ \AA})/\text{Sn}(1 \text{ \AA})/\text{Cu}(15 \text{ \AA})]_{30}$, $[\text{Gd}(100 \text{ \AA})/\text{Cu}(10 \text{ \AA})/\text{Sn}(1 \text{ \AA})/\text{Cu}(30 \text{ \AA})]_{30}$ and $[\text{Gd}(100 \text{ \AA})/\text{Cu}(20 \text{ \AA})/\text{Sn}(1 \text{ \AA})/\text{Cu}(20 \text{ \AA})]_{30}$, respectively. They are practically the same as those of the samples with $t_{\text{Cu}} = 20 \text{ \AA}$.

The series of Mössbauer data gives important information about the magnetism of the Cu layers in the Gd/Cu systems. Although the Gd magnetizations at a certain temperature are different when the position of the ^{119}Sn probes or the thickness of the Cu layer is changed, the

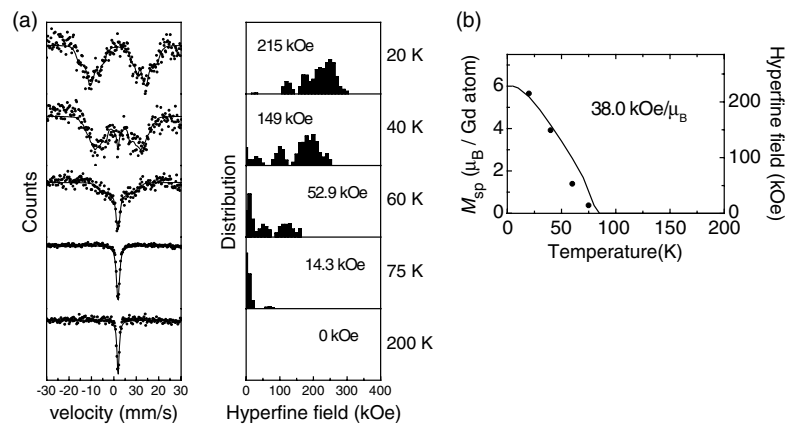


Figure 5. Results of the ^{119}Sn Mössbauer spectroscopy measurements for the sample of $[\text{Gd}(60 \text{ \AA})/\text{Cu}(15 \text{ \AA})/\text{Sn}(1 \text{ \AA})/\text{Cu}(15 \text{ \AA})]$. (a) Temperature dependence of the spectra (circular dots) and fitting curves (solid lines) (left panel), and the hyperfine field distributions obtained from the fittings (right panel). The estimated average hyperfine field at each temperature is also shown. (b) Comparison of the average hyperfine field of Sn (circles) with the spontaneous magnetization of the Gd layer (solid line) at various temperatures. The proportional constant obtained from the least-squares fitting is shown.

proportionality between the average hyperfine field of Sn and the spontaneous magnetization of Gd is always established. The proportional relation allows us to compare the size of Cu magnetic polarization in terms of the hyperfine field per Gd magnetization. The depth profiles of the scaled magnetic polarization obtained from the results on several Gd/Cu multilayers are summarized in figure 7. For all samples with different position of ^{119}Sn probes or different Cu thicknesses, the value of the hyperfine field per Gd magnetization is practically the same, $\sim 40 \text{ kOe}/\mu_{\text{B(Gd)}}$, suggesting that the scaled magnetic polarization of the Cu layers in the Gd/Cu systems is homogeneous, even when the Cu thickness becomes thicker, and reaches 40 Å. We found a relatively narrow distribution of the hyperfine field at 20 K from Mössbauer spectra of a series of the Gd/Cu samples. This fact also supports the homogeneous magnetic polarization at any depth in the Cu layers. Otherwise, a rather broad distribution of the Sn hyperfine field would be observed, because not all ^{119}Sn atoms are necessarily in the same depth due to the interface roughness or intermixing. Indeed, very broad distributions of hyperfine field were observed in Co/Au(Sn) and Fe/Au(Sn) systems [15].

The result that the magnetic polarization in the Cu layers is homogeneous is consistent with a theoretical study on fcc $[\text{Gd}(9 \text{ ML})/\text{Cu}(7 \text{ ML})]$ multilayers by Minár *et al* [19]. They found that a magnetic moment of about $0.0022 \mu_{\text{B}}$ is induced on the interfacial Cu atoms. Moreover, a magnetic moment of the same order of magnitude was found even in the middle of the Cu layers. They conclude that the magnetic moment on the Cu atoms is not induced by the hybridization of the Cu 4p states with the localized 4f states of Gd, but mostly by the hybridization with the 5d states of Gd. The homogeneous magnetic polarization of the Cu layer is in contrast with the case of general (3d magnetic)/(3d nonmagnetic) multilayers, in which the magnetic moment of the nonmagnetic layer seems to concentrate mostly near the interface. The first-principles calculation performed by Samant *et al* [9] suggests that a magnetic moment of the order of $0.01 \mu_{\text{B}}$ is induced in the sp and d bands of the interfacial Cu layer in $[\text{Co}(3 \text{ ML})/\text{Cu}(7 \text{ ML})]$. The size is sharply reduced from the second monolayer.

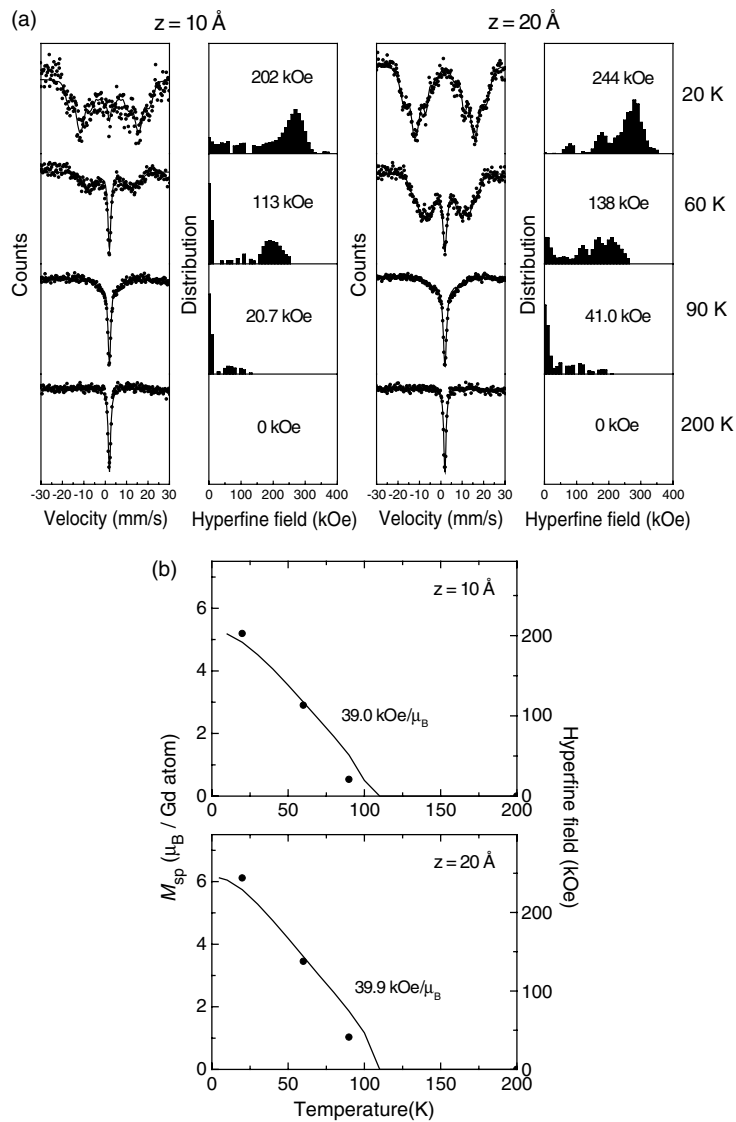


Figure 6. Similar plots to those in figure 4 for the samples $[\text{Gd}(100 \text{ \AA})/\text{Cu}(z)/\text{Sn}(1 \text{ \AA})/\text{Cu}(40 \text{ \AA} - z)]$ with $z = 10$ and 20 \AA .

5. Summary

We performed ^{119}Sn Mössbauer measurements on Gd/Cu multilayers with ^{119}Sn probes embedded in various depths in the Cu layers. We found that large hyperfine fields are induced in the Sn nuclear sites below the Curie temperature of the Gd layer, indicating an existence of magnetic polarization in the Cu layers. The average hyperfine field per Gd magnetization was $\sim 40 \text{ kOe}/\mu_{\text{B(Gd)}}$ at all temperatures below T_C , regardless of the depth of ^{119}Sn from the Gd/Cu interface and of the Cu thickness from 20 to 40 \AA . The results show that the Cu layers in the Gd/Cu system have uniform size of induced magnetic moment.

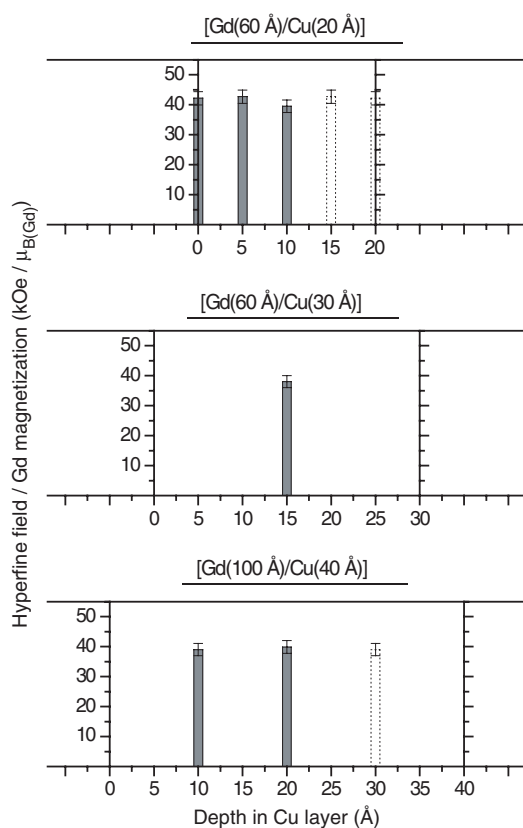


Figure 7. Distribution of the scaled magnetic polarization of the Cu layers in Gd/Cu multilayers estimated from the average hyperfine field at the Sn probes per Gd magnetization. The dotted bars are drawn assuming symmetrical magnetic polarizations in the Cu layers.

Acknowledgments

We thank Mr Y Hayasaki for his support in data collection of XMCD and Mr H Shimizu for the analysis of the EXAFS spectrum. Work at the Advanced Photon Source at Argonne was supported by the US Department of Energy, Office of Science, under contract W-31-109-ENG-38. The XMCD experiments were performed at the BL39XU in the SPring-8 with the approval of the Japan Synchrotron Radiation Institute (JASRI) (Proposal No. 2003B0435-NSc-np). The work was financially supported by a Grant-in-Aid for COE Research ('Elements Science' No. 12CE2005) from the Ministry of Education, Culture, Sports, Science, and Technology of Japan, and a Grant-in-Aid for Scientific Research (No. 13640361) from the Japan Society for the Promotion of Science.

References

- [1] Majkrzak C F, Cable J W, Kwo J, Hong M, McWhan D B, Yafet Y, Waszczak J V and Vettier C 1986 *Phys. Rev. Lett.* **56** 2700
- [2] Binasch G, Grünberg P, Saurenbach F and Zinn W 1989 *Phys. Rev. B* **39** 4828
- [3] Parkin S S P, Bhadra R and Roche K P 1990 *Phys. Rev. Lett.* **66** 2152

-
- [4] Johnson M T, Purcell S T, McGee N W E, Coehoon R, aan de Stegge J and Hoving W 1992 *Phys. Rev. Lett.* **68** 2688
- [5] Edwards D M, Mathon J, Muniz R B and Phan M S 1991 *Phys. Rev. Lett.* **67** 493
- [6] Bruno P and Chappert C 1991 *Phys. Rev. Lett.* **67** 1602
- [7] Ortega J E and Himpsel F J 1992 *Phys. Rev. Lett.* **69** 844
- [8] Koike K, Furukawa T, Gameron G P and Murayama Y 1994 *Japan. J. Appl. Phys.* **33** L769
- [9] Samant M G, Stöhr J, Parkin S S P, Held G A, Hermsmeier B D, Herman F, van Schilfgaarde M, Duda L-C, Mancini D C, Wassdahl N and Nakajima R 1993 *Phys. Rev. Lett.* **72** 1112
- [10] Pizzini S, Fontaine A, Giorgetti C, Dartyge E, Bobo J-F, Picuch M and Baudelet F 1994 *Phys. Rev. Lett.* **74** 1470
- [11] Goto A, Yasuoka H, Yamamoto H and Shinjo T 1993 *J. Phys. Soc. Japan* **62** 2129
- [12] Luetkens H, Korecki J, Morenzoni E, Prokscha T, Birke M, Glückler H, Khasanov R, Klaus H-H, Ślezak T, Suter A, Forgan E M, Niedermayer Ch and Litterst F J 2003 *Phys. Rev. Lett.* **91** 017204
- [13] Ishimatsu N, Hashizume H, Hamada S, Hosoi N, Nelson C S, Venkataraman C T, Srajer G and Lang J C 1999 *Phys. Rev. B* **60** 9596
- [14] Hayasaki Y, Ishiji K, Hashizume H, Hosoi N, Omote K, Kuribayashi M, Srajer G, Lang J C and Haskel D 2004 *J. Phys.: Condens. Matter* **16** 1915
- [15] Emoto T, Hosoi N and Shinjo T 1998 *J. Magn. Magn. Mater.* **189** 136
- [16] Shinjo T, Emoto T, Kawawake Y, Mibu K and Hosoi N 1995 *J. Magn. Magn. Mater.* **140–144** 619
- [17] Ohkochi T, Hosoi N, Mibu K and Hashizume H 2004 *J. Phys. Soc. Japan* **73** 2212
- [18] Vas'kovskiy V O, Svalov A V, Gorbunov A V, Schegoleva N N and Zadvorkin S M 2002 *Physica B* **315** 143
- [19] Minár J, Perlov A, Ebert H and Hashizume H, unpublished